

Micro Electromechanical Filters for Signal Processing

Liwei Lin*, Clark T.-C. Nguyen, Roger T. Howe, and Albert P. Pisano*

Dept. of Electrical Engineering and Computer Sciences

*Dept. of Mechanical Engineering

Berkeley Sensor & Actuator Center

University of California at Berkeley

Berkeley, California 94720 U.S.A.

Abstract

Micro electromechanical filters based on coupled, lateral microresonators are demonstrated. This new class of MEMS has potential signal-processing applications for filters which require narrow bandwidth (high Q), good signal-to-noise ratio, and stable temperature and aging characteristics. Both series and parallel filters have been fabricated and tested using an off-chip modulation technique. The frequency range of these filters is from approximately 5 kHz to on the order of 1 MHz, for polysilicon microstructures with suspension beams having a 2 μm square cross section. A series-coupled resonator pair, designed for operation at atmospheric pressure, has a measured center frequency of 18.7 kHz and a bandwidth of 1.2 kHz.

I. Introduction

The use of electromechanical filters for signal processing dates to the 1940s. In early filters, steel plates were used as the resonators and wires were used as the mechanical coupling elements [1]. Mechanical filters were refined between 1950 to 1970 into effective signal processing components and were designed into a variety of applications [2-4].

Mechanical filters are used where narrow bandwidth, low loss, and good stability are required. They typically have high quality factors (Q), combined with excellent aging characteristics. Figure 1 describes the application domain of mechanical filters, in contrast to other filter types [4]. In present-day mechanical filters, nickel-iron alloys are used in constructing the resonant elements, which are capable of quality factors ranging from 10 000 to 25 000 [4]. Piezoelectric crystals, such as are commonly used in oscillators, are also sometimes used in mechanical filters.

Mechanical filters have been displaced in audio-frequency applications by the advent of integrated switched-capacitor filters, which are implemented in MOS technologies [5]. In addition, integrated analog-to-digital and digital-to-analog converters have made digital filtering attractive in some applications. Where their special properties were not essential, mechanical filters were non-competitive because of higher manufacturing cost and larger size (typically cylinders several cm in length and approximately 1 cm in diameter). With the advent of CMOS VLSI technology, it became feasible to integrate switched-capacitor filters with other functional blocks to fabricate single-chip microsystems (e.g., in a one-chip modem).

If a filter using micromechanical elements could be fabricated using IC processes, then many of their technological drawbacks would be eliminated. In particular, micromechanical filters could emerge as functional blocks in integrated microsystems. Somewhat similar motivations were behind efforts at Westinghouse Research and Development Center in the 1960s to develop micromechanical resonant structures for filtering and

other applications [6]. The pioneering "resonant gate transistor" was a field-effect transistor with a vibrating metal beam replacing the gate. The beam was resonated vertical to the substrate using electrostatic forces applied by an underlying electrode. Typical dimensions of the metal thin-film beams were 0.1 mm long and 5-10 μm thick. Typical quality factors were 500 at 5 kHz. The project was abandoned due to low Q 's, high temperature coefficients of the resonant frequency, and aging of the metal films. In addition, the non-linear electrostatic drive would impose severe constraints on the amplitude of the input signal and thus, the dynamic range of the filter.

Recent advances in micromachining processes and in microresonator materials and design [7,8], have motivated us to reexamine the feasibility of integrated micromechanical filters. Microresonators fabricated from polycrystalline silicon (a low-loss material), driven by interdigitated electrodes (which provide a linear excitation), and suspended by folded flexures (for a linear spring-rate to very large displacements) are very attractive as building blocks for mechanical filters. In addition, laterally driven structures benefit from having all critical features defined in one masking level, which enables the designer to implement such features as differential drive and split combs for levitation suppression, without the need for process changes [9]. To be generally useful, these micromechanical structures must be fabricated together with associated microelectronic interface circuits. A combined CMOS/polysilicon microstructure process is under development at the Berkeley Sensor & Actuator Center [10].

This paper presents the design techniques, microstructural layout, and test results for two basic filter classes based on lateral

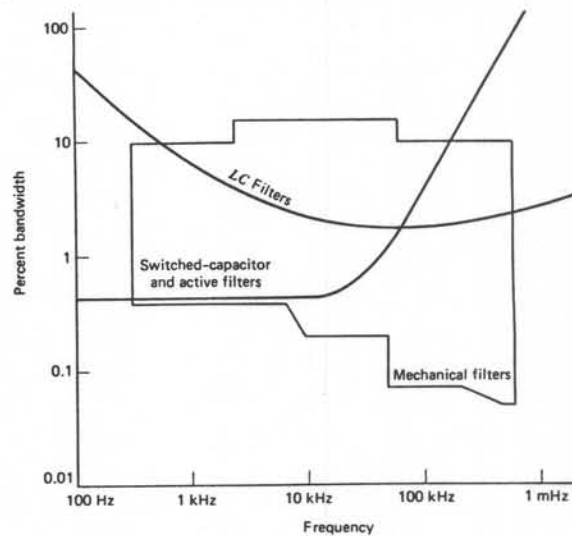


Fig. 1. Application range of LC, active, and switched-capacitor filters in comparison to mechanical filters [4].

polysilicon microresonators: series resonators with mechanical coupling, and parallel resonators with electrically summed responses. Both approaches show promise for achieving high signal-to-noise ratio (with on-chip detection circuits) and quality factors on the order of 50 000 in vacuum. Initial tests at atmospheric response of both filter types are reported. The control of resonant frequencies is a major manufacturing challenge. In conclusion, we discuss techniques and research directors for developing trimming procedures.

II. Filter Topologies

A. Series Micromechanical Filters

The principle of a series mechanical filter is illustrated in Fig. 2, which shows relatively weak springs K_{ij} linking two adjacent resonators having masses M_i , M_j and springs K_i , K_j . In contrast to the frequency response of the uncoupled single resonators, the filter in Fig. 1 can be configured to have an improved bandpass characteristic by proper selection of resonators, coupling springs and bridging springs which link non-adjacent resonators (note that bridging springs have not been drawn in Fig. 2). Hence, higher-order systems with multiple coupling springs enable synthesis of high quality bandpass filters.

Signals, in the form of current or voltage, are converted by an input electromechanical transducer into mechanical vibrations at the filter, pass through the series filter, and are then converted back into electrical signals by an output electromechanical transducer. Magnetostrictive and piezoelectric transducers are commonly used in conventional mechanical filters [4].

The series filter concept has been implemented by using coupled, electrostatically driven polysilicon resonant structures. Figure 3 shows a series two-resonator filter, with a square truss coupling spring. The input and output electrostatic combs function as linear electromechanical transducers, as long as they are biased at a DC voltage which is much larger than the amplitude of the signal voltage [8].

B. Parallel Micromechanical Filters

An electromechanical filter may also be realized by combining the the current outputs of two (or more) microresonators with resonance frequencies, f_1 and f_2 , which differ by a specific, designed amount. Figure 4 shows how this technique, combined with appropriate control of the phase of microresonator motional currents, can be used to realize either a bandpass filter or a notch filter.

For the case of the bandpass filter (Fig. 5 (a)), the relative phase difference between microresonators is selected such that currents combine in the interval between the two resonances (currents are in phase) but subtract outside this interval (currents are approximately 180° out of phase). The notch filter of Fig. 5 (b) is realized with the opposite phasing.

For a flat, symmetrical bandpass response, the resonators should be designed with identical 3dB bandwidths and resonance amplitudes. The frequency separation, $f_2 - f_1$, required for a flat passband response may then be determined by equating the output current seen at the center frequency with the maximum (resonance) current of the individual resonators. From such an analysis, the required frequency separation is found to equal the 3dB bandwidth of the individual resonators constituting the filter:

$$\Delta f = \frac{f_1}{Q_1}, \quad (1)$$

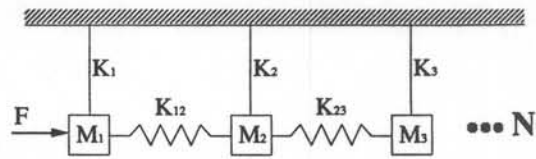


Fig. 2. Conceptual diagram of a coupled series N-resonator filter.

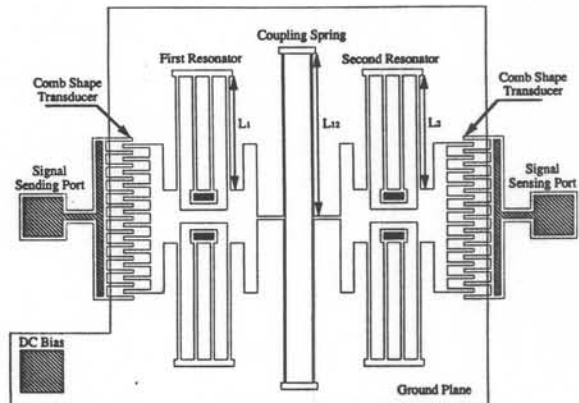


Fig. 3. Schematic diagram of a series two-resonator micro filter.

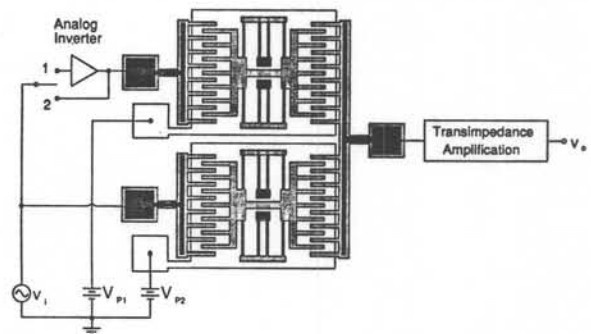


Fig. 4. Schematic of a parallel microresonator filter. When the switch is set at 1, the analog inverter provides a 180° phase shift and a bandpass filter results. When the switch is set at 2, a notch filter is implemented.

where f_1 is the resonance frequency of the lower resonator. The filter rolloff outside the passband specifies the quality factor required of the individual resonators. The combination of a steep rolloff and a relatively broad passband, $f_u - f_l$, therefore demands a large number, N , of resonators in parallel, since:

$$N = \frac{f_u - f_l}{\Delta f} = Q_1 \frac{f_u - f_l}{f_1}. \quad (2)$$

III. Theoretical Response

A. Mechanical Model

The general N-resonator series filter with nearest-neighbor coupling springs can be modeled mechanically as shown in Fig. 6. The transfer function of the output displacement, X_n , to the input force, F , is essential, since the derivative of the output displacement is proportional to the sense current [7]. The transfer function can be expressed as:

$$\frac{X_n}{F} = \frac{1}{C_{2n} S^{2n} + C_{2n-1} S^{2n-1} + C_{2n-2} S^{2n-2} + \dots + C_0} \quad (3)$$

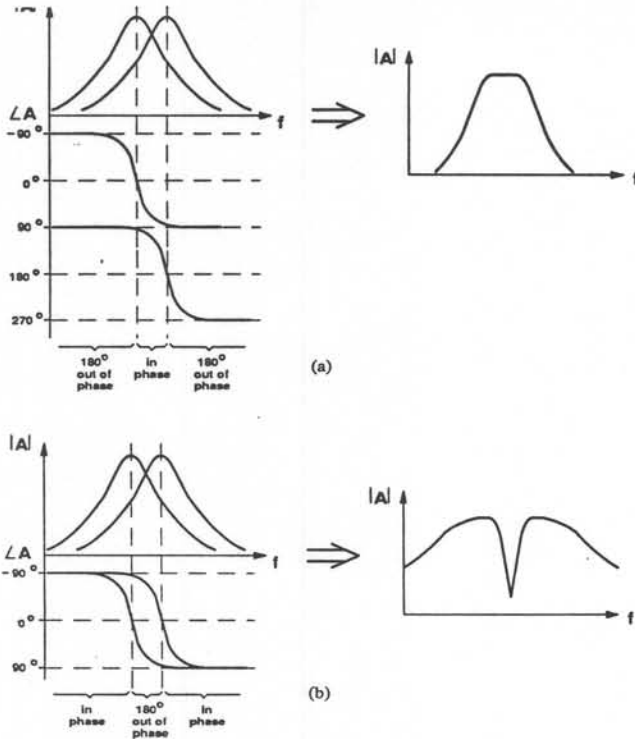


Fig. 4. Schematic of a parallel microresonator filter. When the switch is set at 1, the analog inverter provides a 180° phase shift and a bandpass filter results. When the switch is set at 2, a notch filter is implemented.

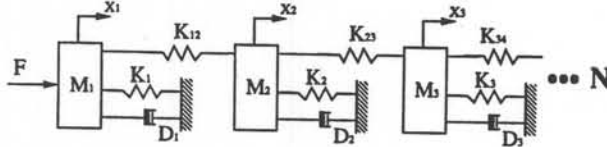


Fig. 6. Mechanical model for a series N-resonator filter. M represents mass, K represents spring constant and D represents damping ratio. Note, the general case of adding bridging springs has not been considered here.

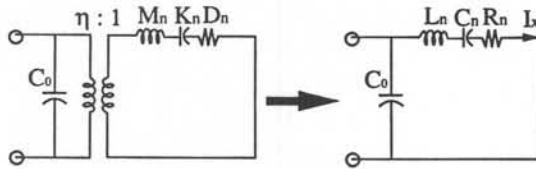


Fig. 7. The equivalent circuit for a comb shape transducer.

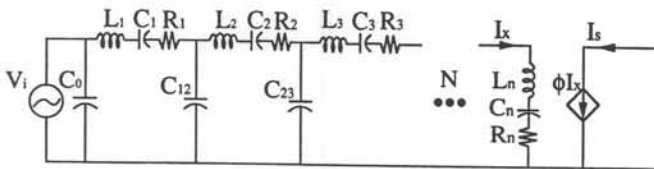


Fig. 8. The equivalent circuit for a series N-resonator filter.

The equivalent mass, spring rate, and damping coefficient for the individual resonators are given by [7]:

$$M_i = M_{ip} + 0.3714M_{ib} \quad (4)$$

$$K_i = 2Eh \left(\frac{W_i}{L_i}\right)^3 \quad (5)$$

$$D_i = \frac{(M_i K_i)^{1/2}}{Q_i} \quad (6)$$

where M_{ip} and M_{ib} represent the mass of the plate and the mass of the folded beams of the i -th resonator, and W_i and L_i are the width and length of the eight struts in its folded suspension. The thickness of the microstructure is h and the Young's modulus is E . The damping coefficient is determined experimentally from the measured quality factor, Q_i , although a reasonable model based on viscous drag has been developed [7]. Quality factors range from less than 100 at atmospheric pressure in air to approximately 50 000 in high vacuum [8].

The inter-resonator coupling spring rates are given by:

$$K_{ij} = Eh \left(\frac{W_{ij}}{L_{ij}}\right)^3, \quad (7)$$

in which W_{ij} and L_{ij} are the width and length of the square truss coupling spring as illustrated in Fig. 3.

From an electronic system design standpoint, the transfer function relating i input voltage to o output current I_o/V_i is most useful. Such a relation may be obtained by relating the internal mechanical parameters, F and X_n , to the corresponding electrical input and output through the phasor relations [11]:

$$F = V_{Pi} \left(\frac{\partial C}{\partial x}\right)_i V_i \quad (8)$$

$$I_o = V_{Po} \left(\frac{\partial C}{\partial x}\right)_o j \omega X_n \quad (9)$$

where V_{Pi} and V_{Po} represent the dc bias at the drive (input) and sense (output) ports, respectively, V_d is the amplitude of the ac driving voltage, and $(\partial C/\partial x)_i$ and $(\partial C/\partial x)_o$ are the capacitive changes with respect to comb motion at the respective ports. For the particular case of comb driven transducers, the value $\partial C/\partial x$ is a constant and can be theoretically approximated (and underestimated, since fringing fields are neglected) [11] as:

$$\frac{\partial C}{\partial x} = \frac{2N \epsilon_0 h}{d} \quad (10)$$

In Eq.(10), where N is the number of the comb fingers, ϵ_0 is the permittivity and d is the gap between the fingers. Hence, the filter transconductance can be expressed in phasor form as:

$$\frac{I_o}{V_i} = \frac{j \omega V_{Pi} V_{Po} \left(\frac{\partial C}{\partial x}\right)_i \left(\frac{\partial C}{\partial x}\right)_o}{C_{2n}(j\omega)^{2n} + C_{2n-1}(j\omega)^{2n-1} + C_{2n-2}(j\omega)^{2n-2} + \dots + C_0} \quad (11)$$

B. Electrical Model

Most previous analyses for filters in the macro scale use the analogy modeling method to transform mechanical elements into equivalent electrical elements in order to apply the large body of electrical filter design tools. The theoretical transformation parameter, η , (shown in Fig. 7(a) for a comb-shaped transducer) can be theoretically obtained by first deriving the equivalent RLC circuit elements for a single comb-driven resonator [11], then generalizing the resulting η for the case of a complete filter. From the above, one finds

$$\eta = \frac{1}{V_{Pi} \left(\frac{\partial C}{\partial x}\right)_i} \quad (14)$$

Table I lists of the indirect analogy between electrical and mechanical systems. Note that force and velocity in a mechanical system can be treated as voltage and current in an electrical system. Hence, the electrical equivalent circuit for the series N-resonator filter in Fig. 6 can be further illustrated in Fig. 8 for a purely electrical model including two transducers. (C_0 is the d.c. capacitance of the comb fingers.) The electrical elements are related to the mechanical elements as follows:

$$L_i = M_i \eta^2 \quad (15)$$

$$C_i = \frac{1}{K_i \eta^2} \quad (16)$$

$$R_i = D_i \eta^2 \quad (17)$$

$$C_{ij} = \frac{1}{K_{ij} \eta^2} \quad (18)$$

The theoretical form of I_x (as defined in Fig. 8) can be derived by pure electrical analysis [11] and the amplification factor, ϕ_i , in Fig. 8 can be expressed as

$$\phi_i = \frac{I_o}{I_x} = \frac{V_{Po} \left(\frac{\partial C}{\partial x} \right)_o}{V_{Pi} \left(\frac{\partial C}{\partial x} \right)_i} \quad (19)$$

The final form of I_o/V_i is exactly the same as Eq.(11).

Table I.
Indirect Analogy between Mechanical and Electrical Systems

| Mechanical System | Electrical System |
|-------------------------------------|-------------------|
| Force(F) | Voltage(V) |
| Velocity($\partial x/\partial t$) | Current(I) |
| Compliance(1/K) | Capacitance(C) |
| Damping(D) | Resistance(R) |
| Mass(M) | Inductance(L) |

C. Electronic Drive and Sense

One method for sensing the output current of an electrostatic comb driven microfilter involves capacitive detection using a depletion mode NMOS transistor [14]. Since the equivalent output resistance of a microresonator is very large (on the order of 10 M Ω), only current noise is important for determination of signal-to-noise ratio. The signal-to-noise ratio can be estimated by using the typical noise characteristics of an MOS transistor [5] and the typical output current of an interdigitated comb [8]. For a filter with a 3 Hz bandwidth, a center frequency of 20 kHz, and a 10 nA output current at resonance, the signal-to-noise ratio (S/N) is calculated to be 146 dB. For wider bandwidths, the S/N degrades with the square root of the pass band. For example, a 1 kHz bandwidth corresponds to an S/N of 120 dB.

In addition to the transimpedance amplifier at the output, an electronic interface could prove useful at the input to the filter. One approach to protecting the filter is to provide some form of automatic gain control at the input. For example, an out-of-range input voltage could be attenuated, input to the mechanical filter, and then re-amplified at the output. There are more ambitious applications involving the electronic control of the characteristics of the mechanical filters. For example, a set of electrically-isolated comb fingers could be used to implement "active damping" in which a voltage which 90° out of phase with the displacement is generated. The electrostatic force from these comb fingers simulates a viscous drag on the resonator and could be used to actively control the quality factor, Q.

IV. Fabrication and Measurements

These filters have been fabricated via the polysilicon surface micromachining process previously used for lateral resonators [7,8], with a polysilicon thickness of approximately 2 μm . The folded suspensions are 2 μm wide, whereas the more compliant coupling springs are only 1 μm wide. All key structures such as the comb, the folded beam resonators, and the coupling springs have been defined and etched in a single masking step. An LPCVD oxide non-erodible etch mask has been used to achieve nearly vertical polysilicon sidewalls. Scanning-electron micrographs (SEMs) of a two-resonator series filters are shown in Fig. 9.

The electrical responses of the fabricated prototype filters have been measured using an off-chip modulation sensing technique [9,11], and in air the single microresonator quality factor is about 30. Table II shows the designed and measured dimensions of the series and parallel filters. Figure 10 shows both the response of a two-resonator series micro filter (with coupling spring length of 150 μm) and the theoretical result. A stiffer coupling spring can produce a wider bandwidth but also increase the passband ripple. Figs. 11 and 12 show the bandpass and notch parallel filters, respectively. Table III illustrates the performance of these filters. All of these spectra show marked improvement over that for a single microresonator, shown in Fig. 13.

Levitation of the comb resonators has caused problems for the operation of the micro filters especially for the series filters. When both sides of the comb structures are levitated, the center part of the filter was deflected downward and dimples on the resonator plates contact the substrate and stop the filter. Levitation can be effectively suppressed by an electrostatically balanced comb structure [9], or by operating at reduced DC bias voltages.

Young's modulus has been determined experimentally by measuring the resonance of single resonators and a value of 150 GPa has been determined. These filters has been designed to operate in air, the separation between two designed resonance frequencies is relatively large (e.g. 1.4 kHz for the type series filter). However, when these filters operated in a vacuum, the quality factor, Q, becomes large and the flat bandpass becomes two separate peaks. Thus, the filters need to be redesigned for operation in vacuum.

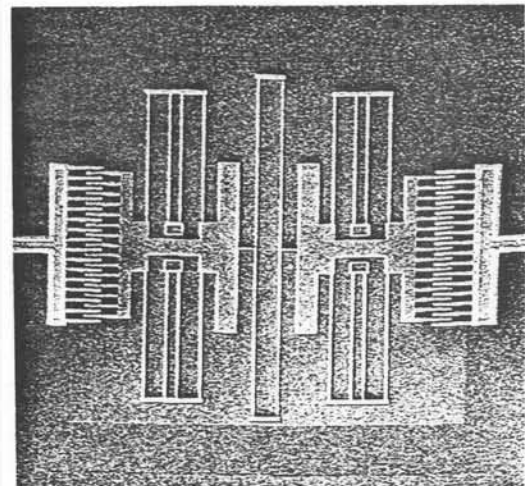


Fig. 9. The SEM photo of a series two-resonator filter.

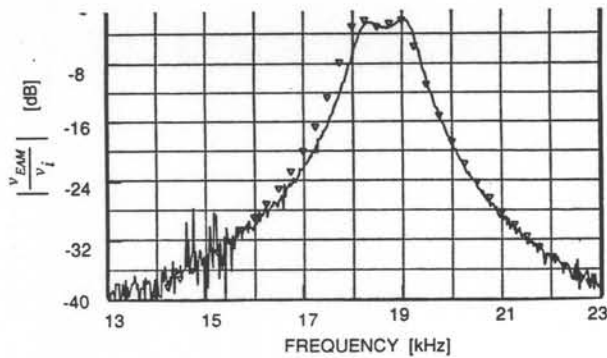


Fig. 10. Measured and theoretical () frequency response spectrum for a series two-resonator bandpass filter.

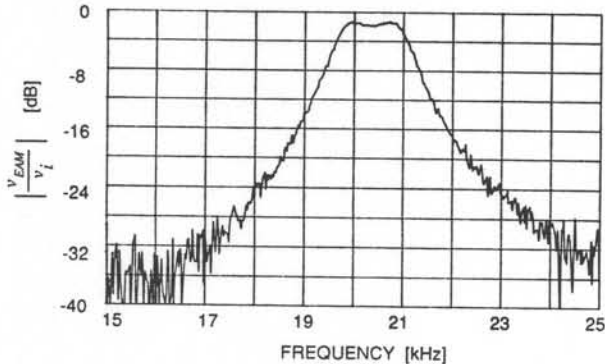


Fig. 11. Measured frequency response spectrum for a parallel two-resonator bandpass filter.

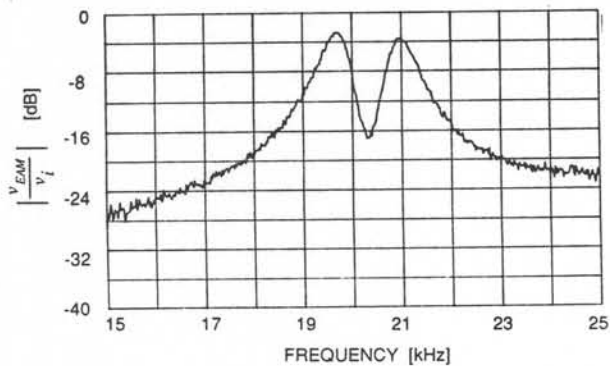


Fig. 12. Measured frequency response spectrum for a parallel two-resonator notch filter.

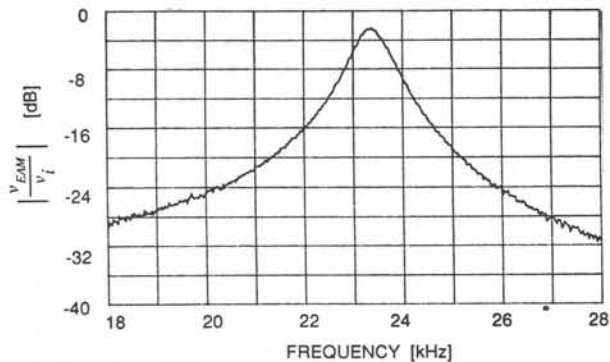


Fig. 13. Measured frequency response spectrum for a single microresonator.

TABLE II.

Dimensions of Tested Series and Parallel Micro Filters
()--measured

| dimensions | Series Filter | Parallel Filter |
|--|---------------|-----------------|
| Number of resonators | 2 | 2 |
| Beam length(resonator #1)[μm] | 150(150) | 200(200) |
| Beam length(resonator #2)[μm] | 150(150) | 195(195) |
| Beam width[μm] | 2(1.7) | 2(2) |
| Thickness[μm] | 2(1.8) | 2(2) |
| Spring length(μm) | 150(150) | - |
| Spring width(μm) | 1(0.8) | - |

Table III.

Characteristics of Tested Series and Parallel Micro Filters

| Characteristics | Series Filter (Fig.10) | Parallel Filter (Fig.11) |
|---|---------------------------|-----------------------------|
| Center frequency (f_o) [KHz] | 18.7 | 20.3 |
| 3dB bandwidth (BW_3) [KHz] | 1.2 | 1.5 |
| 20dB bandwidth(BW_{20}) [KHz] | 3.2 | 4.1 |
| Fractional bandwidth ($\frac{BW_3}{f_o}$) | 6.4% | 7.4% |
| Passband ripple [dB] | 1.5 | 0.5 |
| Shape factor ($\frac{BW_{20}}{BW_3}$) | 2.7 | 2.7 |
| Quality factor ($\frac{f_o}{BW_3}$) | 15.6 | 13.5 |
| Dimensions [mm^2] | 0.032 | 0.032 |

V. Discussion and Conclusions

The initial results indicate that micro electromechanical filters are a promising direction for high-Q, narrowband signal processing. However, there are several technical obstacles to developing practical implementations of these filters. We provide a perspective on the materials, packaging, and manufacturing issues in this section.

The prototype filters are fabricated from LPCVD polycrystalline silicon, which is well-known for having a process-dependent residual strain. The folded suspensions used for the prototype resonators have spring rates which are nearly insensitive to the average residual strain (tensile or compressive) in the film, since they are able to release stress being freed from the substrate [8,15]. The square-truss coupling springs are attached to the resonators at their centerpoints. Therefore, they are also free to expand or contract after removal of the sacrificial layer. A second benefit of folded suspensions is that they largely isolate the filter from strains in the substrate caused by thermal expansion or packaging. Aging should be less of a problem with micro electromechanical filters than with conventional mechanical filters, since polysilicon is a high-Q material.

The filter characteristics are a function of the Young's modulus and the density of polysilicon, both of which vary with temperature. For low-temperature polysilicon, the calculated temperature coefficient of Young's modulus for microcrystalline silicon is $-75 \text{ ppm}/^\circ\text{C}$ [16]. For linear microresonators with folded-beam suspensions, the temperature coefficient of the resonance frequency, TC_f , can be determined by differentiating with respect to temperature, T , yielding an expression of the form $TC_f = \frac{1}{2}(TC_E + TC_h)$, where TC_E and TC_h are the temperature coefficients of the Young's modulus and thickness ($2.5 \text{ ppm}/^\circ\text{C}$ [17], respectively). This predicts a TC_f of $-36 \text{ ppm}/^\circ\text{C}$, which is better than that for conventional mechanical filters, $60 \text{ ppm}/^\circ\text{C}$ [4]. However, the temperature coefficient of frequency

of packaged resonators must be measured in order to make a fair comparison.

Although the initial test devices for both filter types are fabricated by polysilicon, other process sequences and materials are possible and may have advantages for particular applications. For example, single-crystal silicon lateral resonant microstructures identical in design have recently been fabricated by means of a wafer-bonding process [18,19]. A major advantage of the polysilicon structures is that they can be fabricated along with microelectronic functional blocks, as demonstrated by in a recently announced commercial accelerometer [20].

In order to achieve high quality factors, micromechanical filters must be packaged in a moderate to high vacuum. A vacuum ambient could be provided by a hermetic package, although this approach would involve greater cost. Recent progress in micro-encapsulation has demonstrated that the entire filter could be fabricated inside a thin-film vacuum cavity [21,22]. For the relatively small cost of a few additional deposition and masking steps, micromechanical filter chips could be fabricated with no need for special and expensive hermetically-sealed packages.

Conventional mechanical filters require the manufacturing of resonators, coupling wires and transducers, as well as bonding, and final trimming. For micro electromechanical filters, the IC batch process is used to fabricate the resonators, coupling elements, and electronic interface together, thereby achieving the advantages of batch fabrication and avoiding time-consuming steps, such as the serial bonding of coupling wires to resonators. However, the IC process is not sufficiently well controlled that the microresonators can be fabricated without some means of trimming for final adjustment of the filter characteristics. In order to trim the resonant frequencies, processes for adding or removing material from the resonator must be developed. Some options for trimming are laser etching or laser-induced local deposition [23], similar processes using focused ion beams, or the laser-induced evaporation of metal films deposited on the resonator.

In conclusion, this paper has demonstrated the concept of micro electromechanical bandpass filters for audio-frequency applications. In addition to being a new technology for fabricating mechanical filters, there may be potential for developing functional blocks which can be used in integrated microsystems. A modular approach to integrating polysilicon microstructures with CMOS electronics is a prerequisite for developing the devices into a major application of MEMS [24].

Acknowledgements

These devices were fabricated in the UC Berkeley Microfabrication Laboratory. This work has been supported by the Berkeley Sensor & Actuator Center, an NSF/Industry/University Cooperative Research Center.

References

- [1] R. Adler, "Compact electromechanical filters", *Electronics*, 20, pp. 100-105, April 1947.
- [2] J.C. Hathaway, D.F. Babcock, "Survey of Mechanical Filters and Their Applications", *Proc. IRE*, 45, pp. 5-16, Jan. 1957.
- [3] R. A. Johnson, Manfred Borner and Masashi Konno, "Mechanical Filters - A Review of Progress", *IEEE Trans. Sonics Ultrason.*, SU-18, pp. 155-170, July 1971.
- [4] R. A. Johnson, *Mechanical Filters in Electronics*, (New York: John Wiley and Sons, Inc.), 1983.
- [5] R. Gregorian and G. C. Temes, *Analog MOS Integrated Circuits for Signal Processing*, (New York: John Wiley and Sons, Inc.), 1986.
- [6] H. C. Nathanson, W. E. Newell, R. A. Wickstrom and J. R. Davis, "The Resonant Gate Transistor", *IEEE Trans. on Electron Devices*, ED-14, 117-133, March 1967.
- [7] W. C. Tang, T.-C. H. Nguyen, and R. T. Howe, "Laterally Driven Polysilicon Resonant Microstructures", *Sensors and Actuators*, 20, 25-32, 1989.
- [8] W. C. Tang, T.-C. H. Nguyen, M. W. Judy, and R. T. Howe, "Electrostatic-Comb drive of Lateral Polysilicon Resonators," *Sensors and Actuators*, A21-A23, 1990, pp. 328-331.
- [9] W. C. Tang, M. G. Lim, and R. T. Howe, "Electrostatically Balanced Comb Drive for Controlled Levitation," *IEEE Solid-State Sensor and Actuator Workshop*, June 1990, pp. 23-27.
- [10] W. Yun, W. C. Tang, and R. T. Howe, "Fabrication Technologies for Integrated Microdynamic Systems," (invited paper), *Integrated Micro-Motion Systems - Micromachining, Control and Applications*, edited by F. Harashima. Amsterdam: Elsevier Science Publishers, 1990.
- [11] C. T.-C. H. Nguyen, "Electromechanical Characterization of Microsensors for Circuit Applications," M.S. Report, Dept. of Electrical Engineering and Computer Sciences, University of California at Berkeley, April 1991.
- [12] Leonard Meirovitch, *Analytical Methods in Vibrations* (London: The Macmillany Company), 1967.
- [13] Samuel Seely, *Electromechanical Energy Conversion* (New York: McGraw-Hill Company, Inc.), 1962.
- [14] M. W. Putty, et al, "One-Port Active Polysilicon Resonant Microstructures," *IEEE Micro Electro Mechanical Systems Workshop*, Salt Lake City, 1989, pp. 60-65.
- [15] R. I. Pratt, G. C. Johnson, R. T. Howe and J. C. Chang, "Micromechanical Structures for Thin Film Characterization," *Transducers'91*, 205-208, San Francisco, June 1991.
- [16] H. Guckel, et al, "The mechanical properties of fine-grained polysilicon: the repeatability issue," *Technical Digest, IEEE Solid-State Sensor and Actuator Workshop*, Hilton Head Island, S.C., June 1988, pp. 96-99.
- [17] R. S. Muller and T. I Kamins, *Device Electronics for Integrated Circuits*, (New York: John Wiley and Sons, Inc.), 1986.
- [18] K. Suzuki and H. Tanigawa, "Alternative Process for Silicon Linear Micro-Actuators," *Proceedings, 9th Sensor Symposium, IEE Japan*, Tokyo, June 1990, pp. 125-128.
- [19] K. Suzuki, "Single-Crystal Silicon Micro-Actuators," *Technical Digest, IEEE International Electron Devices Meeting*, San Francisco, Calif., December 10-14, 1990, pp. 625-628.
- [20] R. S. Payne and D. A. Dinsmore, "Surface Micromachined accelerometer: a technology update," *Proceedings, SAE Symposium*, Detroit, Michigan, Feb. 1991, pp. 127-135.
- [21] H Guckel, J. J. Sniegowski, T. R. Christenson and F. Raissi, "The Application of Fine-grained, Tensile Polysilicon to Mechanically Resonant Transducers," *Sensors and Actuators*, A21-A23, 1990, pp. 346-351.
- [22] K. M. McNair, "Microstructure Micropackaging," M.S. Report, Dept. of Electrical Engineering and Computer Sciences, University of California at Berkeley, November 1991.
- [23] T. M. Bloomstein and D. J. Ehrlich, "Laser Deposition and Etching of Three Dimensional Microstructures," *Transducers'91*, 507-511, San Francisco, June 1991.
- [24] W. Yun, W. C. Tang, and R. T. Howe, "Fabrication technologies for integrated microdynamic systems," *Technical Digest, The Third Toyota Conference on Integrated Micro Motion Systems*, Nissin, Aichi, Japan, Oct. 22-25, 1989, pp. 17-1 — 17-15.